Chemical Science

ROYAL SOCIETY OF CHEMISTRY

EDGE ARTICLE

View Article Online
View Journal | View Issue

Cite this: *Chem. Sci.*, 2024, **15**, 6445

All publication charges for this article have been paid for by the Royal Society of Chemistry

Received 20th February 2024
Accepted 27th March 2024

DOI: 10.1039/d4sc01188k

rsc.li/chemical-science

Wetting-enhanced adhesion of photo-polymerized supramolecular adhesives for both smooth and rough surfaces†

Mengyuan Zhao,[a] Jiang Wu,[a] Fanxuan Zeng,[a] Zhi Dong,[a] Xinyi Shen,[a] Zan Hua *[b] and Guangming Liu *[a]

Efficient interactions between an adhesive and a substrate surface at the molecular level are the basis for the formation of robust adhesion, which substantially relies on interfacial wetting. However, strong adhesives usually improve cohesion but compromise interfacial properties. Herein, we have reported a kind of robust supramolecular adhesive based on the outstanding mobility and interfacial wettability of adhesive precursors. *In situ* fast photopolymerization endows supramolecular adhesives with more outstanding adhesion for both smooth and rough surfaces in air and underwater in contrast to their counterparts from thermal polymerization. In addition to their low viscosity and high monomer concentration, supramolecular adhesive precursors without any organic solvents possess well-defined hydrogen bonding interactions. These superior properties consistently contribute to the wetting of the substrate and the formation of adhesive polymers with high molecular weights. This work highlights that enhancing interfacial wetting between an adhesive and a substrate is a promising route to achieving robust adhesion.

Introduction

Adhesives are ubiquitous in both daily life and industrial applications and enable bonding between two similar or dissimilar materials.[1,2] The successful application of adhesives is mainly based on building efficient adhesion between the adhesive and the substrate surface at the molecular level.[3] Therefore, the initial interfacial wetting is substantially essential for the formation of adhesion.[4] Common adhesives are able to achieve efficient adhesion in dry environments but undergo failure underwater or under wet conditions.[5–8] The interfacial water layer prevents intimate contact between the substrate and the adhesive, hindering the formation of strong adhesion.[9,10] Additionally, substrate surfaces are often variable, including different surface topographies and distinct roughnesses. Notably, uncontrolled environments such as variable humidity and surface conditions are often unavoidable for the practical application of adhesives, limiting the fabrication of robust adhesion.[11–13] As a result, it is highly desirable to develop new strategies to overcome the current challenge of conventional adhesives.

The main ingredients of adhesives are usually composed of either polymers, or monomers and pre-polymers which can form polymers. For example, pressure-sensitive adhesives (PSAs) as a family of polymers achieve instantaneous adhesion to a variety of surfaces within short contact time and at low contact pressure.[14–16] They basically rely on specific viscoelastic properties of polymers without undergoing any phase transitions or chemical reactions.[17] The macroscopic properties of PSAs are determined by the molecular weight and chain entanglement of the polymers.[18] Although previous work has investigated the effect of surface roughness on PSAs' adhesion behaviors thermodynamically,[19] highly viscous polymeric adhesives make their penetration or wetting to the substrate kinetically slow under application conditions. The difficulty is also encountered for other hydrogel-based or hot-melt polymeric adhesives.[20–24] As such, the application of polymer-based adhesives is seriously restricted especially for rough surfaces.

Alternatively, adhesives from low viscous monomers and pre-polymers could efficiently wet both smooth and rough surfaces. Subsequent *in situ* curing with a combination of superb interfacial wetting provides a feasible approach to the construction of strong adhesives.[25–27] For instance, the commercial Super Glue consists of a series of cyanoacrylate monomers, presenting as liquids with high fluidity prior to use. Subsequently, anionic polymerization initiated by water in the

[a]*Department of Chemical Physics, Key Laboratory of Surface and Interface Chemistry and Energy Catalysis of Anhui Higher Education Institutes, Hefei National Research Center for Physical Sciences at the Microscale, University of Science and Technology of China, Hefei, Anhui, 230026, China. E-mail: gml@ustc.edu.cn*

[b]*The Key Laboratory of Functional Molecular Solids, Ministry of Education, Department of Materials Chemistry, School of Chemistry and Materials Science, Anhui Normal University, Wuhu, Anhui, 214002, China. E-mail: zanhua23@ahnu.edu.cn*

† Electronic supplementary information (ESI) available. See DOI: https://doi.org/10.1039/d4sc01188k

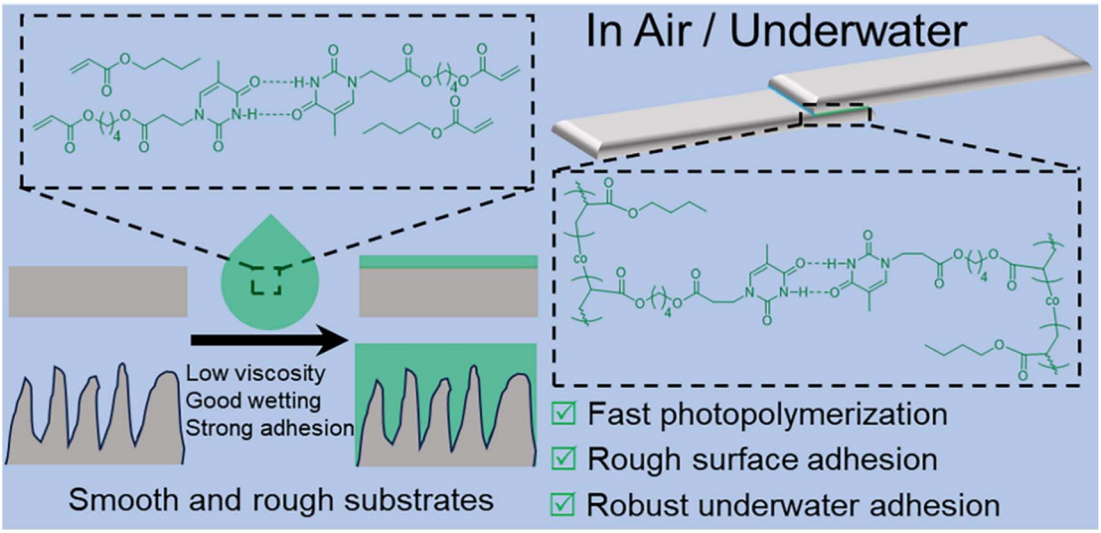

Scheme 1 Schematic illustration of the fabrication of strong adhesion for both smooth and rough surfaces in air and underwater.

environment leads to the formation of strong adhesives with an adhesion strength as high as 10 MPa.[28] However, uncontrolled polymerization conditions make adhesives ineffective underwater or at high humidity.[27,29] In contrast, photopolymerization through the radical process is much more robust, which is compatible with distinct aqueous conditions. The high efficiency of photopolymerization also enables us to achieve control over the reaction spatiotemporally, which is of great importance for fabricating transparent multilayer materials.[30–33] The superb adhesion of these transparent materials is the basis for their widespread applications ranging from functional coatings and optical instruments to solar photovoltaic applications. It should be noted that photopolymerizable adhesives are different from photoswitchable adhesives. Some interesting work about photoswitchable adhesives shows that the reversible change in the polymer structure upon light irradiation gives rise to the change in adhesion.[34,35] In contrast, photopolymerizable adhesives undergo *in situ* efficient polymerization from the monomer to the polymer for achieving adhesion. Yet, it is still challenging to construct outstanding photo-polymerized adhesives with strong adhesion for both smooth and rough surfaces.

Recently, nucleobase-containing adhesives have attracted a lot of attention,[36,37] as they are capable of forming efficient bonding with various substrates through multiple supramolecular interactions, including hydrogen bonding, metal coordination, hydrophobic interactions, and so on. Herein, we have reported a new strategy for achieving strong adhesion for both smooth and rough surfaces in air and underwater by taking full advantage of interfacial wetting properties and supramolecular interactions of nucleobases (Scheme 1). Supramolecular adhesive precursors without any organic solvents have well-defined hydrogen bonding interactions, presenting good mobility and interfacial wettability. *In situ* fast photopolymerization enables us to fabricate supramolecular adhesives with more outstanding adhesion both in air and underwater in contrast to their counterparts from thermal polymerization. The low viscosity and high monomer concentration of supramolecular precursors not only facilitate the wetting of the substrate, but also are beneficial for the formation of adhesive polymers with high molecular weights. The advantages of current supramolecular adhesives are applicable to both smooth and rough surfaces of different materials such as poly(tetrafluoroethylene) (PTFE), poly(methyl methacrylate) (PMMA), poly(ethylene terephthalate) (PET), steel, and ceramics. This work demonstrates the significance of interfacial wetting for the formation of strong adhesion, opening up a unique avenue for designing robust adhesives.

Results and discussion

Synthesis and characterization of photo-polymerized supramolecular adhesives

Photopolymerization is an efficient approach to producing polymers. In contrast to methacrylate and methacrylamide-type monomers, acrylate-type monomers possess a faster polymerization kinetics owing to their higher propagation rate constant, facilitating fast fabrication of adhesives. Initially, *n*-butyl acrylate (*n*BA) was selected to explore the photo-polymerization kinetics using 2, 2-dimethoxy-2-phenylacetophenone (DMPA, 1 wt%) as the photo-initiator with a distance of 10 cm between the light source and the reaction mixture. The light source is composed of 6 × 8 W lamps with a central wavelength of 365 nm. ^{1}H NMR spectra showed that the conversion of *n*BA increased rapidly to *ca.* 80% after 2 min (Fig. S1†). Afterwards, a slow increase was observed, achieving a conversion of as high as 92% within 5 min (Fig. S2†). A further increase in irradiation time only gives rise to a slight increase in monomer conversion. Therefore, we would use the optimized polymerization conditions, *i.e.* 1 wt% photoinitiator and a photoirradiation of 5 min for further *in situ* construction of supramolecular adhesives.

Since the homopolymer P*n*BA is not sticky enough to be used as an adhesive, thymine-containing monomer, 4-((3-(thymidin-

1-yl)propanoyl)oxy)butyl acrylate (TAc), was prepared and copolymerized to tackify the photo-polymerized adhesives (Scheme S1, Fig. S3 and S4†).[38–40] Although thymine typically forms hydrogen bonds with the complementary nucleobase adenine, thymine–thymine non-complementary hydrogen bonding is often observed in the biological system as well such as the wobble region in tRNA recognition.[41] Initially, the hydrogen bonding interactions of TAc were characterized by using ^{1}H NMR spectroscopy (Fig. 1a). By using the external reference method, we investigate the formation of hydrogen bonding between TAc monomers in the monomer mixtures of *n*BA and TAc without any solvents. With the molar ratio of *n*BA and TAc decreasing from 12 : 1 to 3 : 1, the peak at 10.86 ppm assigned to the proton connected to N3 in thymine gradually shifts to 11.10 ppm, which can be caused by the formation of thymine–thymine hydrogen bonds (Fig. 1a). The protons involved in the formation of hydrogen bonds in thymine give rise to a decrease in electron density, displaying the low-field shift. Meanwhile, the proton at 7.87 ppm attributed to the thymine also presents a gradual increase with the increase in the molar ratio of TAc in the supramolecular mixture. In stark contrast, no obvious changes were observed for other protons, which are far from the hydrogen bond-forming moieties (Fig. S5†). Collectively, these results illustrate that efficient hydrogen bonding for TAc was formed in the supramolecular mixture.

Furthermore, a series of supramolecular copolymers PL_{x-y} were obtained after photoirradiation for 5 min, in which x and y represent the molar ratio between *n*BA and TAc, respectively (Scheme S2†). The UV-vis spectra of the supramolecular mixtures of *n*BA and TAc monomers with and without the photoinitiator were measured. The results show that the supramolecular mixtures without the photoinitiator have low absorbance over the wavelength of 300 nm (Fig. S6†). In contrast, with the addition of 1 wt% of the photoinitiator, a new peak of absorption was observed at around 350 nm. Notably, the UV-vis measurements were conducted with the supramolecular mixtures without solvent in a cuvette of 1 mm optical length, which is over 100 times thicker than that of the formed adhesive. Therefore, UV-irradiation at 365 nm can efficiently pass through the supramolecular mixtures to form adhesives. As shown in Fig. 1b, Fourier transform infrared (FT-IR) spectra of the copolymers show the full disappearance of the carbon–carbon double bond stretching vibration at 1650–1620 cm^{-1} for all copolymers. Therefore, high conversions for all copolymers from PL_{12-1} to PL_{3-1} were achieved. In addition, the absorbance at 1675 cm^{-1} for C=O stretching vibration of amide presents a gradual increase from PL_{12-1} to PL_{3-1}, suggesting that more TAc monomers were copolymerized in the copolymers. Thermal properties of the resulting copolymers were characterized by thermogravimetric analysis (TGA) and differential scanning calorimetry (DSC). All attained copolymers display good thermal stability with decomposition temperatures over 318.9 °C (Fig. S7†). The DSC curves of all copolymers showed a single glass transition temperature (T_g) ranging from −32.1 °C for PL_{12-1} to −3.4 °C for PL_{3-1}, indicating that random copolymers were formed (Fig. 1c). The increase of thymine in the copolymers leads to a linear increase in T_g, which should be due to the hydrogen bonding between thymine (Fig. S8†).

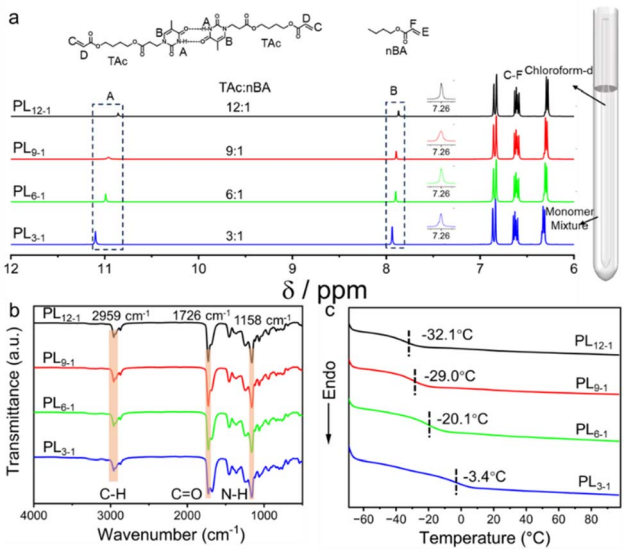

Fig. 1 Molecular characterization and thermal analyses of nucleobase-containing copolymers. (a) ^{1}H NMR spectra of *n*BA and TAc monomer mixtures at different molar ratios with $CDCl_3$ in the interior tube. (b) FT-IR spectra and (c) DSC curves of P(*n*BA-*co*-TAc) copolymers through photo-polymerization.

Adhesive properties of supramolecular thymine-containing polymers

Adhesive properties of photopolymerized thymine-containing copolymers were investigated through shear tests. Two clean glass slides were coated and bonded with a thin layer of monomer mixtures. The lap joint area was controlled to be 1.0 cm^2 (2.5 cm × 0.4 cm) and exposed to photoirradiation for 5 min. The shear strengths were observed to gradually increase from 2.04 ± 0.62 MPa for PL_{12-1} to 3.81 ± 0.49 MPa for PL_{3-1} (Fig. 2a). It should be noted that photopolymerization of P*n*BA only gives a polymer with a low shear strength of 0.06 MPa (Fig. S9†). Therefore, the robust adhesion of supramolecular adhesives should be caused by the strong intermolecular and intramolecular hydrogen bonds of thymine. Since cohesion failure was observed for all these copolymers, the increase in adhesion strengths from PL_{12-1} to PL_{3-1} should be attributed to stronger intermolecular H-bonding interactions from higher contents of thymine.

To further unravel the reason for the strong adhesion of photopolymerized supramolecular adhesives, thymine-containing copolymers were also prepared through thermal polymerization initiated by 2,2′-azobis(2-methylpropionitrile) (AIBN) in *N*,*N*-dimethylformamide (DMF) solution (Scheme S3†). Copolymers from PT_{12-1} to PT_{3-1} produced through thermal polymerization have the same chemical compositions as copolymers from PL_{12-1} to PL_{3-1} through photo-polymerization. Meanwhile, the thermal properties of the copolymers present no discernible difference for the

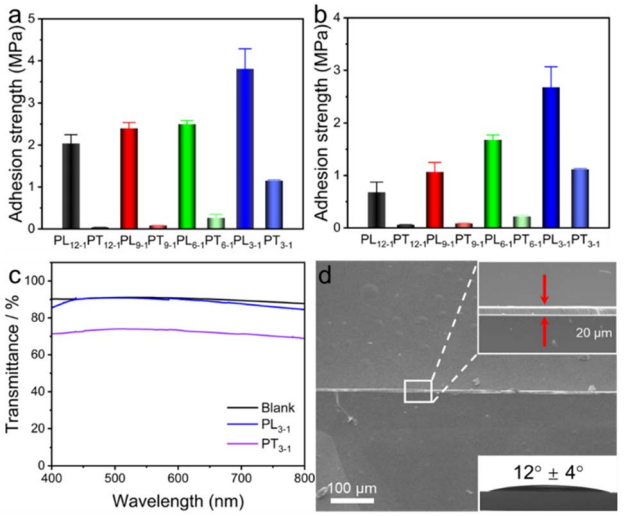

Fig. 2 Adhesion properties of the P(*n*BA-*co*-TAc) copolymers from either photo or thermal polymerization. Adhesion strengths of supramolecular adhesives from photopolymerization from PL_{12-1} to PL_{3-1} and thermal polymerization from PT_{12-1} to PT_{3-1} on smooth glass slides (a) in air and (b) underwater. (c) UV-vis transmittance of supramolecular adhesive bonded glass slides. (d) SEM image of PL_{3-1} bonded glass slides. The insets show the enlarged interface between two bonded glass slides and the contact angle image of the monomer precursor for PL_{3-1} on a smooth glass slide in air.

copolymers with the same chemical compositions from either photo or thermal polymerizations (Fig. S10–S12†). Intriguingly, the shear strengths of copolymers from PT_{12-1} to PT_{3-1} are 3.4–33.3 times lower than those of photopolymerized copolymers from PL_{12-1} to PL_{3-1} in air (Fig. 2a). Since all the copolymers possess hydrophobicity with water contact angles over 90° (Fig. S13†), they are also suitable for use as underwater adhesives. Likewise, the photopolymerized adhesives present 2.5–7.8 times stronger adhesion than adhesives from thermal polymerization underwater (Fig. 2b). Interestingly, the supramolecular adhesives still present strong adhesion when formed in acidic water. The adhesion properties of PL_{3-1} were tested in solutions at a pH of 3.0 and 5.0 respectively. The results showed that both samples maintained a high adhesion strength of 2.45 ± 0.42 MPa at a pH of 5.0 and 2.21 ± 0.04 MPa at a pH of 3.0 (Fig. S14†). We further tested the contact angle of the PL_{3-1} precursor on glass immersed into aqueous solutions at a pH of 3.0 and 5.0. The results showed that the precursors maintain good hydrophobicity, as the supramolecular precursors and adhesives mainly consisted of hydrophobic *n*BA. Therefore, it is difficult for the acidic aqueous solution to disrupt the hydrogen bonds of thymine, contributing to strong adhesion.

Although both photo and thermal polymerization generate copolymers with substantially the same chemical compositions and thermal properties, their different molecular weights and wetting to substrates are surmised to result in remarkably distinct adhesive properties. In contrast to the copolymers from PT_{12-1} to PT_{3-1} (Fig. S15 and Table S1†), the photopolymerized copolymers are not capable of being dissolved in DMF for size exclusion chromatography (SEC). Considering that the photopolymerization is conducted without solvents, a high monomer concentration is favorable for forming polymers with high molecular weights. Additionally, the preorganized non-complementary H-bonds between TAc monomers are favorable for the intermolecular and intramolecular interactions, limiting their solubility in DMF. More importantly, the wetting of adhesives to substrates is of significance for the formation of robust adhesion. If two transparent substrates were bonded with adhesives uniformly, high transmittance was observed owing to the lack of holes or defects for light scattering. As shown in Fig. 2c, a high transmittance of 90% from 400 to 800 nm was observed for PL_{3-1} bonded glass slides. In contrast, the PT_{3-1} bonded glass slides only give a low transmittance of *ca.* 70% (Fig. 2c). High viscosity of the PT_{3-1} copolymer limits its efficient wetting to the glass slides, leading to the formation of minor holes or defects (Fig. S16†).

The microscopic wetting of the supramolecular adhesive PL_{3-1} to the glass substrates was further investigated. The scanning electron microscope (SEM) image shows that a thin and uniform layer of adhesive was formed between two glass slides (Fig. 2d). The enlarged image indicates that the adhesive has an average thickness of *ca.* 6 μm and is closely attached to both substrates without undulation. Furthermore, we have found that the monomer mixture of precursors has good wetting on the glass substrate with a contact angle of 12° ± 4°, demonstrating excellent wetting. Taken together, the low viscosity and high concentration of the monomer mixture enable efficient wetting to the substrate and fast polymerization, achieving robust adhesion.

Adhesion of supramolecular nucleobase-containing copolymers on rough surfaces

Achieving strong adhesion to rough surfaces is significant but highly challenging. Rough surfaces usually have irregular protrusions and pits, which makes it hard to wet the substrate with the adhesive. The situation is more severe and intractable for highly viscous polymer adhesives with low mobility. As a result, it requires much more time and energy for the fabrication of efficient adhesion to rough substrates. In contrast, the application of high mobile adhesive precursors is feasible to address the above-mentioned issues through the *in situ* formation of supramolecular adhesives. In order to systematically explore the adhesion on rough surfaces, glass slides with various roughnesses were employed as substrates to investigate the performance of supramolecular adhesives.

Surface roughness of the glass was first studied and evaluated by using SEM. The representative SEM image for the rough glass shows many irregular humps and holes ranging from several to tens of micrometers in size (Fig. 3a). Four kinds of rough glass slides were obtained from commercial suppliers, representing different average surface roughnesses (Fig. S17†). In order to compare the adhesion on different rough substrates, the average surface roughness of glass was further quantitatively studied by using an optical profilometer.[42] As shown in Fig. 3b, many protrusions and pits with depths from −7.2 to 5.7 μm were randomly distributed on the rough glass. The average

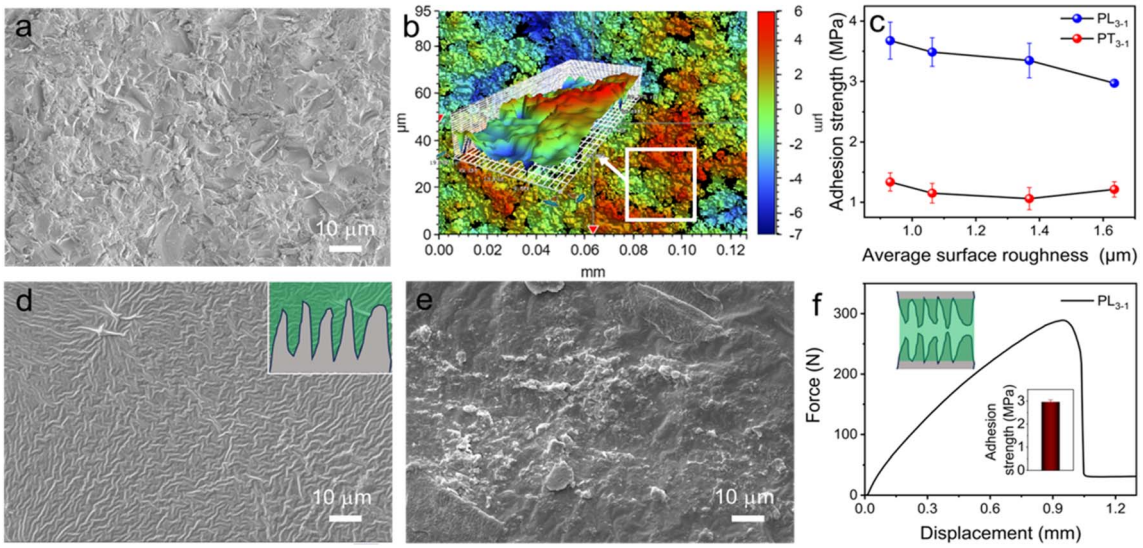

Fig. 3 Adhesion of PL_{3-1} and PT_{3-1} supramolecular adhesives on different rough surfaces. (a) SEM image and (b) optical surface profile of representative rough glass with an average surface roughness of 1.64 μm ± 0.14 μm. The inset in (b) shows the 3D profile of the rough surface. (c) Shear strengths of PL_{3-1} and PT_{3-1} supramolecular adhesives on different rough glasses. SEM images of (d) PL_{3-1} and (e) PT_{3-1} bonded glass surfaces after the shear test with the insets showing the schematic wetting of the adhesive to the substrate. The green and red areas represent PL_{3-1} and PT_{3-1} supramolecular adhesives, respectively. (f) The shear force–displacement curves of two rough substrates bonded with the adhesive PL_{3-1}.

surface roughness (R_{sa}) of the substrate as shown in Fig. 3b is 1.64 μm ± 0.14 μm. Four different rough glasses further studied have R_{sa} values of 0.93, 1.06, 1.37, and 1.64 μm, respectively. The adhesion of both PL_{3-1} and PT_{3-1} adhesives was explored on different rough surfaces by bonding with a smooth glass (Fig. 3c). The PL_{3-1} adhesive is capable of achieving strong adhesion over 3.0 MPa on rough surfaces irrespective of the surface roughness. Specifically, a slight decrease in shear strength was observed from 3.7 MPa for the glass with a R_{sa} of 0.93 μm to 3.0 MPa for that of 1.64 μm. Collectively, the supramolecular adhesive precursor with low viscosity enables efficient wetting to the rough surfaces (Fig. S18†), generating strong bonding through the *in situ* photopolymerization. In contrast, about 3 times lower shear strengths from 1.06 to 1.34 MPa were observed for the PT_{3-1} adhesive. It should be caused by the poor wetting of the highly viscous PT_{3-1} adhesive, giving rise to the poor contact between the adhesive and the rough substrate.

The surface of the rough substrate after the shear test was further studied with SEM imaging as shown in Fig. 3d and e. For the rough glass with a R_{sa} of 1.64 μm, the rough surface bonded with PL_{3-1} presents wrinkles, which should be due to the fracture of the adhesive after the shear test (Fig. 3d). By contrast, the rough surface can still be distinguished when using the adhesive PT_{3-1}, suggesting poor contact between the adhesive and the substrate. More importantly, the supramolecular adhesive PL_{3-1} is also capable of bonding two rough substrates with a shear force as high as 300 N (Fig. 3f). The adhesion strength is *ca.* 3.0 MPa, which can be due to the excellent wetting of the adhesive to the substrate. Indeed, the bonded area was optically transparent (Fig. S19†), indicating that both the rough surfaces were filled with the adhesive homogeneously.

Therefore, the low viscous supramolecular adhesive precursor successfully wet the rough substrates, giving rise to the formation of robust adhesion based on highly efficient photopolymerization.

In situ underwater adhesion of supramolecular adhesives on rough surfaces

The intimate contact between the substrate and water makes underwater adhesion difficult. Water-absorbing hydrogels are often employed for the construction of underwater adhesion. However, the long-standing stability for underwater adhesion is compromised by uncontrolled swelling.[43,44] Alternatively, hydrophobic polymer adhesives are able to expel the water layer, effectively achieving underwater adhesion.[40,45,46] Although the strategy by using hydrophobic polymers works properly for a smooth substrate, it is usually not feasible for a rough surface. Two main factors hinder the applicability of hydrophobic polymer adhesives underwater. First, a rough substrate is full of convex and concave areas with different curvatures, preventing the access of highly viscous polymers. Second, higher energy barriers are required to realize the removal of the interfacial water layer for the rough surface compared with the smooth surface.[47]

Intriguingly, the underwater shear strengths of the supramolecular adhesive PL_{3-1} are all over 1.8 MPa for the glass substrates with different roughnesses (Fig. 4a). For the surface with a R_{sa} of 0.93 μm, the adhesion strength is as high as 2.19 ± 0.06 MPa. When the roughness of the substrate increases, a slight drop in the adhesion strength is observed. By contrast, the adhesive PT_{3-1} from thermal polymerization only gives

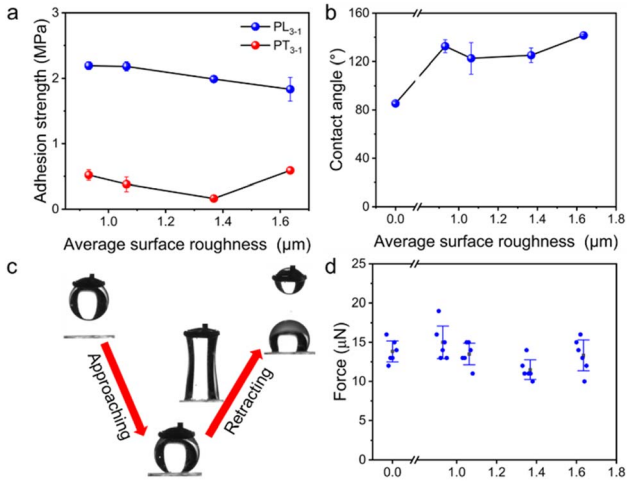

Fig. 4 Underwater adhesion and wettability properties of the supramolecular adhesive PL_{3-1} and the precursor on rough surfaces. (a) Underwater adhesion strengths of PL_{3-1} and PT_{3-1} on glass slides with different roughnesses; (b) underwater contact angle of the PL_{3-1} precursor on glass slides with different roughnesses; (c) the photos taken of the glass slides with a R_{sa} of 1.64 μm approaching and retracting from the representative PL_{3-1} precursor droplet underwater during the measurements of the adhesive force; (d) the measured underwater adhesive forces of the PL_{3-1} precursor on glass slides with different roughnesses.

adhesion strength less than 0.6 MPa. The wettability and the adhesive force of the PL_{3-1} precursor were studied to unveil the mechanism for strong underwater adhesion. As shown in Fig. 4b, the underwater contact angle (CA) of the PL_{3-1} precursor was between 85° and 135° on glass slides with different roughnesses. These results indicate that the wetting of the PL_{3-1} precursor can repel the trapped water in the cavity on the rough glasses.

Similar to apparent contact angles, the microscopic adhesive force explicitly displays the adhesion between the substrate and the supramolecular adhesive precursor, relating to the repellency of the intimate interfacial water layer. Fig. 4c shows that the glass slide with a R_{sa} of 1.64 μm was approaching the PL_{3-1} precursor droplet with a volume of *ca.* 10 μL following the subsequent retraction. The PL_{3-1} precursor liquid was largely stretched and broken from the middle, indicating that the adhesive force of the PL_{3-1} precursor liquid to the substrate is large (Video S1†). The measured adhesive forces are all about 12.0 μN for different rough surfaces (Fig. 4d). As all the droplets were stretched to break from the middle, the actual adhesive force should be greater than the measured value. Collectively, the PL_{3-1} precursor of the supramolecular adhesive possesses strong adhesive forces for different rough glasses. Based on the spontaneous wetting and outstanding underwater adhesion, the hydrophobic PL_{3-1} precursor with low initial viscosity is efficient for the repellency of interfacial water, which lays the foundation for the formation of strong underwater adhesion on rough surfaces. Therefore, *in situ* construction of supramolecular adhesives through photo-polymerization is able to resolve the problem of conventional underwater polymer adhesives.

Robust adhesion of photo-polymerized adhesives on distinct substrates

In situ construction of supramolecular adhesives through photo-polymerization is an efficient and general way to build robust adhesion. To explore the wide range of applicability for supramolecular adhesives, a range of different substrates were used to bond with the glass slide. Strong adhesion was observed to be formed by employing the supramolecular adhesive PL_{3-1} for different smooth substrates both in air and underwater (Fig. 5a). The shear strengths for PL_{3-1} on PTFE, PMMA, PET, steel, and ceramics in air were 0.46, 3.16, 3.55, 3.42, and 3.10 MPa, respectively (Fig. 5a). The strong adhesion can be attributed to multiple intermolecular interactions between the adhesive and the substrate. When the adhesion was conducted underwater, a slight decrease in the adhesion strengths was observed. The adhesion strengths are still over 2.0 MPa for PMMA, PET, steel, and ceramics, showcasing excellent adhesive properties.

The adhesion of the supramolecular adhesive PL_{3-1} on different rough substrates was further investigated (Fig. 5b). Different substrates were abraded to form rough surfaces, which were analyzed by using SEM (Fig. S20†). Strong adhesion was achieved on these rough substrates, displaying adhesion strengths over 1.0 MPa in air. Only a slight drop in the adhesion strength was observed when the adhesive PL_{3-1} was formed underwater (Fig. 5b). The fast and efficient bonding formed by the supramolecular adhesive PL_{3-1} was demonstrated by instantly repairing a leaking water pipeline with the rough surface (Fig. S21†). In contrast, leakage is still observed when using PT_{3-1} under identical conditions. Meanwhile, the bonded sample between glass and steel with the supramolecular adhesive PL_{3-1} can sustain a weight of 2 kg underwater for over 1 h,

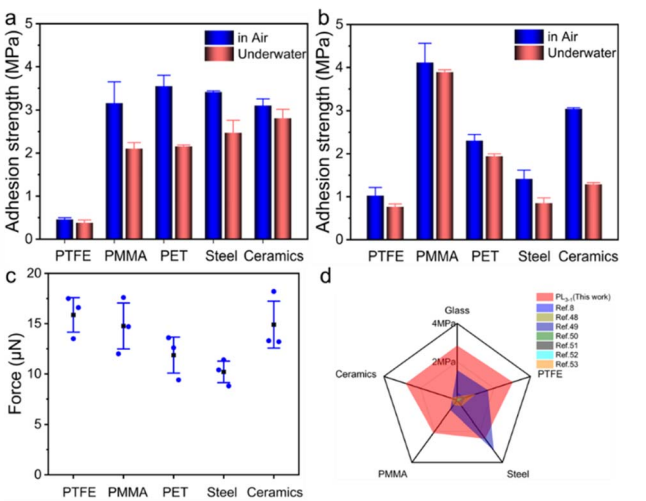

Fig. 5 Properties of photo-polymerized adhesives on distinct substrates. Adhesion strengths of the supramolecular adhesive PL_{3-1} in air and underwater to different (a) smooth and (b) rough substrates, including PTFE, PMMA, PET, steel, and ceramics. (c) The measured underwater adhesive forces of the PL_{3-1} precursor on different rough substrates. (d) Comparison of underwater adhesion strength of the supramolecular adhesive PL_{3-1} with other adhesives.

whereas it undergoes adhesive failure for PT_{3-1} in less than 5 min (Fig. S22†).

The adhesive forces of the PL_{3-1} precursor on different rough surfaces were also measured, showing high adhesive force over 10.2 μN (Fig. 5c). All the PL_{3-1} precursor droplets were stretched to break from the middle, demonstrating strong adhesive force for different rough surfaces underwater. Besides the strong adhesive force, high mobility of the PL_{3-1} precursor also enables efficient wetting to the substrate and the repellency of the interfacial water layer. The photopolymerized supramolecular adhesive is a strong and efficient adhesive underwater, outperforming many polymeric-based underwater adhesives (Fig. 5d).[8,48–53] Thus, a low viscous supramolecular precursor provides us with a straightforward way to fabricate robust underwater adhesion by exploiting spontaneous wetting.

Conclusion

In summary, we have developed an efficient and straightforward method to fabricate outstanding supramolecular adhesives for both smooth and rough surfaces in air and underwater. The supramolecular adhesives can be formed *in situ* through irradiating the supramolecular precursor for 5 min. The supramolecular interaction between thymine-containing monomers without solvents was studied by ^{1}H NMR spectroscopy, indicating the formation of intermolecular hydrogen bonds. The photo-polymerized supramolecular thymine-containing adhesives present 2.5–33.3 times stronger adhesion strengths compared with their counterparts from thermal polymerization for both smooth and rough surfaces. Most importantly, the supramolecular adhesives are capable of achieving robust underwater adhesion on different rough substrates, including PTFE, PMMA, PET, steel, and ceramics. Further study has indicated that the low viscosity and high monomer concentration of the supramolecular precursors are of great significance for the formation of strong adhesion. It is not only beneficial for the formation of adhesive polymers with high molecular weights, but also facilitates the wetting of the substrate and the repellency of the interfacial water layer. All these factors are unanimously in favor of the construction of strong adhesion.

Data availability

The data that support the findings of this study are available from the corresponding author upon reasonable request.

Author contributions

The manuscript was written through contributions of all authors. All authors have given approval to the final version of the manuscript. Z. H. and G. L. conceived the study. M. Z. carried out most of the experiments and analysed the related data. J. W., F. Z., Z. D., and X. S. participated in the experiments for monomer and polymer syntheses.

Conflicts of interest

The authors declare no competing financial interest.

Acknowledgements

This work was financially supported by the National Natural Science Foundation of China (22273098, 22373003, 22103002, and 52033001) and the Fundamental Research Funds for the Central Universities (WK2480000007). This work was partially carried out at the Instruments Center for Physical Science, University of Science and Technology of China.

References

1 H. Cho, G. Wu, J. Christopher Jolly, N. Fortoul, Z. He, Y. Gao, A. Jagota and S. Yang, Intrinsically reversible superglues *via* shape adaptation inspired by snail epiphragm, *Proc. Natl. Acad. Sci. U. S. A.*, 2019, **116**, 13774–13779.
2 C. Cui and W. Liu, Recent advances in wet adhesives: Adhesion mechanism, design principle and applications, *Prog. Polym. Sci.*, 2021, **116**, 101388.
3 G. Raos and B. Zappone, Polymer Adhesion: Seeking New Solutions for an Old Problem, *Macromolecules*, 2021, **54**, 10617–10644.
4 A. Narayanan, A. Dhinojwala and A. Joy, Design principles for creating synthetic underwater adhesives, *Chem. Soc. Rev.*, 2021, **50**, 13321–13345.
5 J. D. White and J. J. Wilker, Underwater Bonding with Charged Polymer Mimics of Marine Mussel Adhesive Proteins, *Macromolecules*, 2011, **44**, 5085–5088.
6 M. A. North, C. A. Del Grosso and J. J. Wilker, High Strength Underwater Bonding with Polymer Mimics of Mussel Adhesive Proteins, *ACS Appl. Mater. Interfaces*, 2017, **9**, 7866–7872.
7 K. Zhan, C. Kim, K. Sung, H. Ejima and N. Yoshie, Tunicate-Inspired Gallol Polymers for Underwater Adhesive: A Comparative Study of Catechol and Gallol, *Biomacromolecules*, 2017, **18**, 2959–2966.
8 C. Wei, X. Zhu, H. Peng, J. Chen, F. Zhang and Q. Zhao, Facile Preparation of Lignin-Based Underwater Adhesives with Improved Performances, *ACS Sustain. Chem. Eng.*, 2019, **7**, 4508–4514.
9 B. K. Ahn, Perspectives on Mussel-Inspired Wet Adhesion, *J. Am. Chem. Soc.*, 2017, **139**, 10166–10171.
10 X. Deng, J. Tang, W. Guan, W. Jiang, M. Zhang, Y. Liu, H. L. Chen, C. L. Chen, Y. Li, K. Liu and Y. Fang, Strong Dynamic Interfacial Adhesion by Polymeric Ionic Liquids under Extreme Conditions, *ACS Nano*, 2022, **16**, 5303–5315.
11 B. N. J. Persson, Biological Adhesion for Locomotion on Rough Surfaces: Basic Principles and A Theorist's View, *MRS Bull.*, 2007, **32**, 486–490.
12 D. R. King, M. D. Bartlett, C. A. Gilman, D. J. Irschick and A. J. Crosby, Creating Gecko-Like Adhesives for "Real World" Surfaces, *Adv. Mater.*, 2014, **26**, 4345–4351.
13 J. Kim, Y. Wang, H. Park, M. C. Park, S. E. Moon, S. M. Hong, C. M. Koo, K. Y. Suh, S. Yang and H. Cho, Nonlinear

Frameworks for Reversible and Pluripotent Wetting on Topographic Surfaces, *Adv. Mater.*, 2016, **29**, 1605078.
14 C. Creton, Pressure-Sensitive Adhesives: An Introductory Course, *MRS Bull.*, 2003, **28**, 434–439.
15 W. Maassen, M. A. R. Meier and N. Willenbacher, Unique adhesive properties of pressure sensitive adhesives from plant oils, *Int. J. Adhes. Adhes.*, 2016, **64**, 65–71.
16 K. H. Park, D. Y. Lee, S. H. Yoon, S. H. Kim, M. S. Han, S. Jeon, Y. Kim, Y. K. Lim, D.-H. Hwang, S.-H. Jung and B. Lim, Adhesion Improvement of Solvent-Free Pressure-Sensitive Adhesives by Semi-IPN Using Polyurethanes and Acrylic Polymers, *Polymers*, 2022, **14**, 3963.
17 S. Mapari, S. Mestry and S. T. Mhaske, Developments in pressure-sensitive adhesives: a review, *Polym. Bull.*, 2020, **78**, 4075–4108.
18 J.-H. Lee, T.-H. Lee, K.-S. Shim, J.-W. Park, H.-J. Kim, Y. Kim and S. Jung, Molecular weight and crosslinking on the adhesion performance and flexibility of acrylic PSAs, *J. Adhes. Sci. Technol.*, 2016, **30**, 2316–2328.
19 H. Guo, M. O. Saed and E. M. Terentjev, Mechanism of Pressure-Sensitive Adhesion in Nematic Elastomers, *Macromolecules*, 2023, **56**, 6247–6255.
20 H. Kasem and M. Varenberg, Effect of counterface roughness on adhesion of mushroom-shaped microstructure, *J. R. Soc., Interface*, 2013, **10**, 20130620.
21 N. Cañas, M. Kamperman, B. Völker, E. Kroner, R. M. McMeeking and E. Arzt, Effect of nano- and micro-roughness on adhesion of bioinspired micropatterned surfaces, *Acta Biomater.*, 2012, **8**, 282–288.
22 G. Moreira Lana, X. Zhang, C. Müller, R. Hensel and E. Arzt, Film-Terminated Fibrillar Microstructures with Improved Adhesion on Skin-like Surfaces, *ACS Appl. Mater. Interfaces*, 2022, **14**, 46239–46251.
23 Y. Zhu, Z. Zheng, Y. Zhang, H. Wu and J. Yu, Adhesion of elastic wavy surfaces: interface strengthening/weakening and mode transition mechanisms, *J. Mech. Phys. Solids*, 2021, **151**, 104402.
24 F. Jin, W. Zhang, Q. Wan and X. Guo, Adhesive contact of a power-law graded elastic half-space with a randomly rough rigid surface, *Int. J. Solids Struct.*, 2016, **81**, 244–249.
25 R. Yang, X. Zhang, B. Chen, Q. Yan, J. Yin and S. Luan, Tunable backbone-degradable robust tissue adhesives *via in situ* radical ring-opening polymerization, *Nat. Commun.*, 2023, **14**, 6063.
26 G. Ge, K. Mandal, R. Haghniaz, M. Li, X. Xiao, L. Carlson, V. Jucaud, M. R. Dokmeci, G. W. Ho and A. Khademhosseini, Deep Eutectic Solvents-Based Ionogels with Ultrafast Gelation and High Adhesion in Harsh Environments, *Adv. Funct. Mater.*, 2023, **33**, 2207388.
27 Y. Liu, G. Guan, Y. Li, J. Tan, P. Cheng, M. Yang, B. Li, Q. Wang, W. Zhong, K. Mequanint, C. Zhu and M. Xing, Gelation of highly entangled hydrophobic macromolecular fluid for ultrastrong underwater *in situ* fast tissue adhesion, *Sci. Adv.*, 2022, **8**, eabm9744.
28 C. R. Westerman, B. C. McGill and J. J. Wilker, Sustainably sourced components to generate high-strength adhesives, *Nature*, 2023, **621**, 306–311.
29 J. Li, A. D. Celiz, J. Yang, Q. Yang, I. Wamala, W. Whyte, B. R. Seo, N. V. Vasilyev, J. J. Vlassak, Z. Suo and D. J. Mooney, Tough adhesives for diverse wet surfaces, *Science*, 2017, **357**, 378–381.
30 X. Deng, L. Mammen, Y. Zhao, P. Lellig, K. Müllen, C. Li, H. J. Butt and D. Vollmer, Transparent, Thermally Stable and Mechanically Robust Superhydrophobic Surfaces Made from Porous Silica Capsules, *Adv. Mater.*, 2011, **23**, 2962–2965.
31 X. Deng, L. Mammen, H.-J. Butt and D. Vollmer, Candle Soot as a Template for a Transparent Robust Superamphiphobic Coating, *Science*, 2012, **335**, 67–70.
32 R. Chen, Y. Zhang, Q. Xie, Z. Chen, C. Ma and G. Zhang, Transparent Polymer-Ceramic Hybrid Antifouling Coating with Superior Mechanical Properties, *Adv. Funct. Mater.*, 2021, **31**, 202011145.
33 Y. H. Chen, C. W. Hwang, S. W. Chang, M. T. Tsai, K. N. Jayakumaran, L. C. Yang, Y. C. Lo, F. H. Ko, H. C. Wang, H. L. Chen and D. Wan, Eco-Friendly Transparent Silk Fibroin Radiative Cooling Film for Thermal Management of Optoelectronics, *Adv. Funct. Mater.*, 2023, **33**, 2301924.
34 K. Imato, K. Momota, N. Kaneda, I. Imae and Y. Ooyama, Photoswitchable Adhesives of Spiropyran Polymers, *Chem. Mater.*, 2022, **34**, 8289–8296.
35 J. J. B. van der Tol, T. A. P. Engels, R. Cardinaels, G. Vantomme, E. W. Meijer and F. Eisenreich, Photoswitchable Liquid-to-Solid Transition of Azobenzene-Decorated Polysiloxanes, *Adv. Funct. Mater.*, 2023, **33**, 2301246.
36 Z. Dong, J. Wu, X. Shen, Z. Hua and G. Liu, Bioinspired nucleobase-containing polyelectrolytes as robust and tunable adhesives by balancing the adhesive and cohesive properties, *Chem. Sci.*, 2023, **14**, 3938–3948.
37 X. Liu, Q. Zhang, L. Duan and G. Gao, Tough Adhesion of Nucleobase-Tackifed Gels in Diverse Solvents, *Adv. Funct. Mater.*, 2019, **29**, 1900450.
38 J. Wu, H. Lei, J. Li, Z. Zhang, G. Zhu, G. Yang, Z. Wang and Z. Hua, Nucleobase-Tackified renewable plant oil-based supramolecular adhesives with robust properties both under ambient conditions and underwater, *Chem. Eng. J.*, 2021, **405**, 126976.
39 S. Cheng, M. Zhang, N. Dixit, R. B. Moore and T. E. Long, Nucleobase Self-Assembly in Supramolecular Adhesives, *Macromolecules*, 2012, **45**, 805–812.
40 J. Wu, H. Lei, X. Fang, B. Wang, G. Yang, R. K. O'Reilly, Z. Wang, Z. Hua and G. Liu, Instant Strong and Responsive Underwater Adhesion Manifested by Bioinspired Supramolecular Polymeric Adhesives, *Macromolecules*, 2022, **55**, 2003–2013.
41 L. J. Voigt, K. E. Tucker and P. M. Zelisko, Thymine-Modified Silicones: A Bioinspired Approach to Cross-Linked, Recyclable Silicone Polymers, *Biomacromolecules*, 2023, **24**, 3463–3471.
42 C. Linghu, Y. Liu, Y. Y. Tan, J. H. M. Sing, Y. Tang, A. Zhou, X. Wang, D. Li, H. Gao and K. J. Hsia, Overcoming the adhesion paradox and switchability conflict on rough

surfaces with shape- memory polymers, *Proc. Natl. Acad. Sci. U. S. A.*, 2023, **120**, e2221049120.

43 X. Ma, X. Zhou, J. Ding, B. Huang, P. Wang, Y. Zhao, Q. Mu, S. Zhang, C. Ren and W. Xu, Hydrogels for underwater adhesion: adhesion mechanism, design strategies and applications, *J. Mater. Chem. A*, 2022, **10**, 11823–11853.

44 S. Wang, J. Liu, L. Wang, H. Cai, Q. Wang, W. Wang, J. Shao and X. Dong, Underwater Adhesion and Anti-Swelling Hydrogels, *Adv. Mater. Technol.*, 2022, **8**, 2201477.

45 L. Yao, C. Lin, X. Duan, X. Ming, Z. Chen, H. Zhu, S. Zhu and Q. Zhang, Autonomous underwater adhesion driven by water-induced interfacial rearrangement, *Nat. Commun.*, 2023, **14**, 6563.

46 C. Fu, L. Shen, L. Liu, P. Tao, L. Zhu, Z. Zeng, T. Ren and G. Wang, Hydrogel with Robust Adhesion in Various Liquid Environments by Electrostatic-Induced Hydrophilic and Hydrophobic Polymer Chains Migration and Rearrangement, *Adv. Mater.*, 2023, 2211237.

47 S. Dalvi, A. Gujrati, S. R. Khanal, L. Pastewka, A. Dhinojwala and T. D. B. Jacobs, Linking energy loss in soft adhesion to surface roughness, *Proc. Natl. Acad. Sci. U. S. A.*, 2019, **116**, 25484–25490.

48 Z. Wang, S. Zhang, S. Zhao, H. Kang, Z. Wang, C. Xia, Y. Yu and J. Li, Facile biomimetic self-coacervation of tannic acid and polycation: Tough and wide pH range of underwater adhesives, *Chem. Eng. J.*, 2021, **404**, 127069.

49 X. Li, Y. Deng, J. Lai, G. Zhao and S. Dong, Tough, Long-Term, Water-Resistant, and Underwater Adhesion of Low-Molecular-Weight Supramolecular Adhesives, *J. Am. Chem. Soc.*, 2020, **142**, 5371–5379.

50 D. Lee, H. Hwang, J.-S. Kim, J. Park, D. Youn, D. Kim, J. Hahn, M. Seo and H. Lee, VATA: A Poly(vinyl alcohol)- and Tannic Acid-Based Nontoxic Underwater Adhesive, *ACS Appl. Mater. Interfaces*, 2020, **12**, 20933–20941.

51 J. Xu, X. Li, J. Li, X. Li, B. Li, Y. Wang, L. Wu and W. Li, Wet and Functional Adhesives from One-Step Aqueous Self-Assembly of Natural Amino Acids and Polyoxometalates, *Angew. Chem., Int. Ed.*, 2017, **56**, 8731–8735.

52 X. Zhu, C. Wei, F. Zhang, Q. Tang and Q. Zhao, A Robust Salty Water Adhesive by Counterion Exchange Induced Coacervate, *Macromol. Rapid Commun.*, 2019, **40**, 1800758.

53 C. Cui, C. Fan, Y. Wu, M. Xiao, T. Wu, D. Zhang, X. Chen, B. Liu, Z. Xu, B. Qu and W. Liu, Water-Triggered Hyperbranched Polymer Universal Adhesives: From Strong Underwater Adhesion to Rapid Sealing Hemostasis, *Adv. Mater.*, 2019, **31**, 1905761.